

Error Mitigation by Restricted Evolution

Gaurav Saxena^{1,*} and Thi Ha Kyaw^{1,†}

¹*LG Electronics Toronto AI Lab, Toronto, Ontario M5V 1M3, Canada*

(Dated: September 11, 2024)

Error mitigation techniques, while instrumental in extending the capabilities of near-term quantum computers, often suffer from exponential resource scaling with noise levels. To address this limitation, we introduce a novel approach, constant runtime Error Mitigation by Restricted Evolution (EMRE). Through numerical simulations, we demonstrate that EMRE surpasses the performance of Probabilistic Error Cancellation (PEC) while maintaining constant sample complexity. Moreover, we uncover a continuous family of error mitigation protocols, Hybrid EMREs (HEMREs), encompassing PEC and EMRE as special cases. HEMREs offer a tunable bias parameter, allowing for a trade-off between sample complexity and error reduction. Thus, our error mitigation protocols provide flexibility in balancing error mitigation with computational overhead, catering to practical application requirements of near-term and early-fault tolerant quantum devices.

I. INTRODUCTION

The practical quantum computational advantage is one of the holy grails that the entire quantum information community aims to achieve. It has recently been pointed out that material science and chemistry are two potential areas of applications where practical quantum advantage might be unleashed [1]. It is believed that such an event will occur at the level of early fault-tolerant quantum computing that involves a substantial number of qubits and quantum gates [2] that the current near-term quantum hardware does not possess. The design of such powerful quantum computers will require sustained effort in the field for a very long time, making the possibility of a “quantum winter” a real concern. In order to sustain the momentum of top-notch research and continual funding support, the quantum information community must show some form of practical quantum advantage [3, 4] using near-term or pre-fault-tolerant quantum hardware.

On the other hand, the near-term quantum hardware is prone to undesired noise. Unlike fault-tolerant quantum algorithms, most near-term quantum algorithms [5–7] are short-depth and come in the form of a hybrid quantum-classical feedback loop. Since quantum circuits do not take up a heavy load in the entire calculation, a higher noise budget is allowed in the hybrid algorithms. A common feature of such hybrid approaches is the variational method [8–12]. Typically, characterizing target quantum systems often involves constructing trial wavefunctions with a substantial yet manageable number of variational parameters. These parameters are then optimized to minimize the energy of the system by invoking a classical computer in the form of a feedback loop. Implicitly, this approach leverages the user’s intuition and knowledge of the target system to select a parameter space that, while extensive, is significantly smaller than the full Hilbert space. The latter, of course, grows exponen-

tially with the number of particles in the system. One major computational routine there is to compute the expectation value of some physical observables [13]. Even with such hybrid quantum-classical algorithms, current noisy quantum hardware could produce unreliable measurement outcomes of the physical observables. What we recently showed in Ref. [14] is that due to the noisy nature of quantum hardware, in order to see some meaningful results in quantum simulations, the quality of the quantum hardware should be below certain gate fidelities, thereby putting a hard limit on the practicality of the noisy devices.

Recently, a handful of quantum error mitigation (QEM) techniques have been proposed [15–27] to improve the expectation values in noisy quantum hardware. The hope is that, with the aid of QEM, one would be able to carry out near-term quantum algorithms effectively without needing to worry about the experimental noises. Intuitively, such an approach would allow us to increase the quantum system size systematically, thereby potentially crossing a threshold where any best classical computing algorithms would not be able to catch up with quantum ones due to either exponentially large Hilbert space or highly entangled many-body quantum ground state structures. Hence, the term “quantum utility era” [28]. A caveat though is that most of the existing quantum error mitigation schemes require either exponential samplings or exponential copies of quantum states, with respect to the amount of noise, to be able to attain resolvable and reliable statistics of the measurement outcome [29]. In fact, there exist universal performance limits such that sampling overhead scales exponentially with the circuit depth given a desired computational accuracy [30]. Even at relatively shallow circuit depth, a superpolynomial number of samplings is needed [31].

Our primary objective is to mitigate the exponential computational overhead associated with quantum error mitigation protocols while preserving reasonable accuracy. Recognizing the inherent trade-off between computational efficiency and statistical precision, we propose methods that intentionally introduce biases into the expectation value estimates. In contrast to probabilistic

* gaurav.saxena@lge.com

† thiha.kyaw@lge.com

error cancellations [16, 17], our approach requires significantly less sampling overhead to achieve comparable results while removing the exponential sampling overhead. In fact, we formally prove that our proposal can estimate expectation values with constant sampling complexity. Moreover, unlike zero-noise extrapolation [15, 16], our techniques avoid extrapolation procedures, thereby eliminating the need for heuristic assumptions.

Here, we develop a constant runtime quantum error mitigation protocol by approximating each noisy quantum gate present in the quantum circuit, thereby restricting the quantum dynamical evolution of the input quantum state. Hence the name error mitigation by restricted evolution (EMRE). The main idea of EMRE is inspired by the generalized robustness measure defined for quantum operations in the context of resource theory of channels [32–35]. At the heart of EMRE, the generalized robustness is used to find the closest (noisy) implementable circuit to the ideal quantum circuit. Using the new implementable circuit, we show that we can estimate the ideal expectation value closely using constant sampling overhead (see Fig. 1 and Sec. III A). The price we pay is that the estimated expectation value comes with a small non-zero bias. We also establish an analytical relationship between the bias and the generalized robustness thus quantifying how bias grows with the noise in the circuit.

The remainder of this paper is organized as follows. In Sec. II, we briefly present the idea of probabilistic error cancellation for the sake of completeness. In Sec. III and Sec. IV, we introduce our two mitigation protocols and analyze how the outputs of the protocol, the expectation value and bias, depend on the decompositions used in the protocols. Sec. III A discusses the measure, the generalized robustness, which quantifies the bias in EMRE. In Sec. III B, we derive bounds on the generalized robustness under different noise models. We present hybrid methods combining PEC and EMRE in Sec. IV. Numerical results are presented in Sec. V. ‘Discussion’ is in Sec. VI where we summarize our work and present some open problems.

II. PRELIMINARIES: PROBABILISTIC ERROR CANCELLATION

Probabilistic Error Cancellation (PEC) is an error mitigation technique that uses the knowledge of the noise occurring in the system to mitigate the errors in estimating quantities such as Born-rule probability or expectation value of an observable. The original idea of PEC proposed in Ref. [16], involved expressing the actual gate in the circuit in terms of (noisy) gates that can be implemented practically. Here, the set of implementable operations refers to the set of noisy operations that can be applied in an actual experimental setup. Such a set can be discrete or continuous. So, if the noise acting in the system is known, one can define the basis set of implementable operations. Based on this set, a quasi-probabilistic decomposition of the actual gate can be

found in terms of the implementable gate sets.

To be explicit, let us consider a single unitary quantum gate U . We are interested in the expectation value of some observable \mathcal{O} , i.e., we want to compute $\text{Tr}[\mathcal{O}\mathcal{U}(|0\rangle\langle 0|)]$ with $\mathcal{U}(\cdot) = U(\cdot)U^\dagger$. Due to the presence of noise \mathcal{E} , we cannot implement U ideally but instead, we implement the noisy U which is $\mathcal{E} \circ U$. Hence, we will end up with $\text{Tr}[\mathcal{O}\mathcal{E} \circ \mathcal{U}(|0\rangle\langle 0|)]$. To mitigate the error using PEC, we first get the decomposition of the gate U in terms of implementable operations. Let $\mathcal{B}_1, \mathcal{B}_2$ be implementable operations (that is, of the form $\mathcal{B}_i = \mathcal{E} \circ \mathcal{U}_i$ where \mathcal{U}_i is some quantum operation), such that $\mathcal{U} = q_1\mathcal{B}_1 - q_2\mathcal{B}_2$, where $q_1, q_2 > 0$ and $q_1 - q_2 = 1$. By using this decomposition, we construct a probability distribution $(q_1/(q_1 + q_2), q_2/(q_1 + q_2))$. We can then sample the gates \mathcal{B}_1 and \mathcal{B}_2 according to this probability distribution, and replace the ideal/desired U in the circuit with these implementable gates. Let the expectation values of the observable \mathcal{O} when using \mathcal{B}_1 and \mathcal{B}_2 be β_1 and β_2 , respectively. Therefore, using β_1 and β_2 , we can compute the actual expectation value as $\text{Tr}[\mathcal{O}\mathcal{U}(|0\rangle\langle 0|)] = q_1\beta_1 - q_2\beta_2$. In the above, we have used a quasi-probabilistic decomposition and it is well known that finding such an optimal decomposition is a hard problem [16, 32] by itself.

For a quantum algorithm with multiple unitary gates, we need to sample many times. By keeping a record of the coefficients and their signs, and by combining them according to the decomposition of every gate in the algorithm, we obtain the *unbiased* expectation value. The sampling size to get the unbiased estimate depends on the product of the absolute sum of the coefficients in the quasi-probabilistic decomposition of each gate in the circuit. It has been shown that sampling overhead increases exponentially with the number of gates in the circuit and the probability of error [16, 29]: $M_{\text{PEC}} = \frac{2\gamma^2}{\epsilon^2} \ln(2/p_{\text{fail}})$, where γ is the robustness (see Sec. III A), ϵ is the precision of the Monte Carlo sampling, and p_{fail} is the probability of failure for the Monte Carlo sampling algorithm. Here, $\gamma \approx e^{4Dp}$ with D being the circuit depth and p being the probability of gate error [29].

III. ERROR MITIGATION BY RESTRICTED EVOLUTION (EMRE)

Although the PEC protocol outputs an unbiased estimate, it does so at an exponential cost, thereby eliminating any potential computational advantage that we might gain from quantum computation. Here, we address this problem by restricting the evolution of a quantum state and present a method to mitigate errors using only *constant sampling overhead*. We coin this protocol: error mitigation by restricted evolution (EMRE). The details are as follows.

Let an n -qubit quantum circuit with depth D be rep-

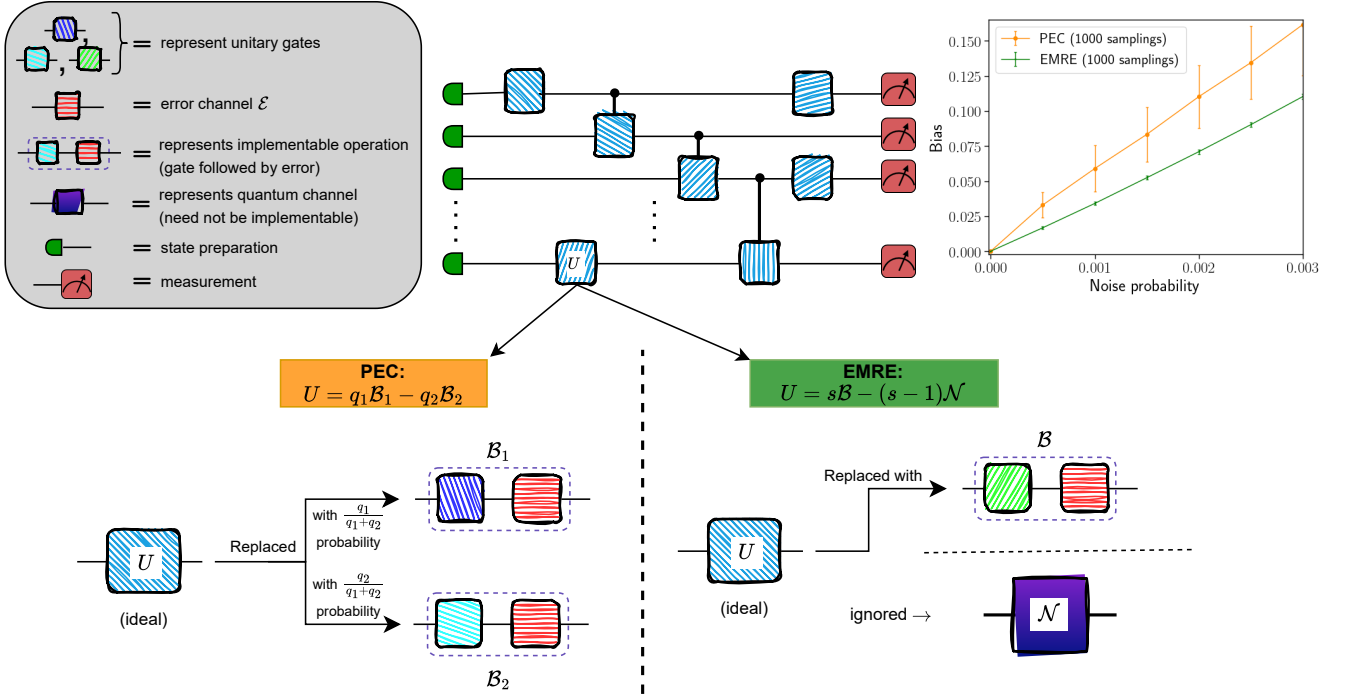


FIG. 1: Illustration of mitigating errors by restricting the evolution of the quantum state, outlining the difference between EMRE and PEC in terms of circuit construction and expected outcomes. Performing error mitigation by restricted evolution (or EMRE) requires a constant sample size as opposed to PEC which has an exponential sampling overhead. In practical applications, PEC is deployed by reducing its sampling size. In such scenarios, we numerically demonstrate that EMRE outperforms PEC as seen in the inset figure where both EMRE and PEC use 1000 samplings. We would like to point out the stability of our proposed EMRE as apparent from very small error bars across different noise probabilities.

resented by \mathcal{U} as

$$\mathcal{U} := \mathcal{U}_D \circ \cdots \circ \mathcal{U}_2 \circ \mathcal{U}_1$$

where each \mathcal{U}_i represents the i th layer of the circuit acting on the n qubits. For each layer, we can find a number $s_i \geq 1$ and an implementable operation \mathcal{B}_i (or a convex combination thereof) such that $s_i \mathcal{B}_i \geq \mathcal{U}_i$, i.e., $s_i J^{\mathcal{B}_i} - J^{\mathcal{U}_i} \geq 0$ where $J^{\mathcal{B}_i}$, $J^{\mathcal{U}_i}$ are the Choi matrices of the operations \mathcal{B}_i and \mathcal{U}_i , respectively. The above inequality implies that there exist a set of quantum channels $\{\mathcal{N}_i\}$ such that for each respective \mathcal{U}_i , it holds that

$$\mathcal{U}_i = s_i \mathcal{B}_i - (s_i - 1) \mathcal{N}_i. \quad (1)$$

The optimal $s_i - 1$ can be thought of as the generalized robustness, inspired by the generalized robustness measure from dynamical resource theories [32–35]. (In-depth discussions on the generalized robustness are provided in Secs. III A and III B.) Let us call the decomposition in Eq. (1) as the generalized quasi-probability decomposition where the terms with negative coefficients need not be implementable operations. By using the above decomposition for all gates in the circuit, we can represent the whole circuit \mathcal{U} as follows

$$\mathcal{U} = s \mathcal{B} - (s - 1) \mathcal{N} \quad (2)$$

where

$$s = \prod_{i=1}^D s_i, \quad (3)$$

$$\mathcal{B} = \mathcal{B}_D \circ \cdots \circ \mathcal{B}_2 \circ \mathcal{B}_1, \quad (4)$$

and \mathcal{N} is the quantum channel that consists of all other combinations. Using this decomposition, we aim to output an estimate E of the expectation value $\text{Tr}[\mathcal{O} \mathcal{U}(|0\rangle\langle 0|)]$ of some observable \mathcal{O} such that

$$|E - \text{Tr}[\mathcal{O} \mathcal{U}(|0\rangle\langle 0|)]| \leq b, \quad (5)$$

where b represents a small bias.

To reduce the sampling overhead to estimate the expectation value E , we approximate each unitary \mathcal{U}_i with $s_i \mathcal{B}_i$. Practically, this means that we replace the i -th operation (or the i -th layer) in the circuit with \mathcal{B}_i and multiply the estimate after the measurement with s_i (see Fig. 1). Therefore, we approximate the whole circuit with implementable operations as follows:

$$\mathcal{U} \approx s \mathcal{B} = s \mathcal{B}_D \circ \cdots \circ \mathcal{B}_2 \circ \mathcal{B}_1. \quad (6)$$

Approximating the circuit in this way, we can say that we restrict evolving the input state under the ideal circuit \mathcal{U} to the implementable circuit \mathcal{B} . The price we pay is that

the bias b in Eq. (5) will always be finite which comes from the approximation of \mathcal{U} in Eq.(6) by restricting the unitary circuit with an implementable (noisy) circuit. The proposed algorithm can be considered a direct application of the classical simulation algorithm presented in Ref. [36]. Next, we discuss in detail how to estimate the expectation value E and the bias b from the above approximation (also refer to Fig. 2).

Let $c \ll 1$ be a fixed small positive constant. Using the Monte Carlo samplings of various \mathcal{B}_i 's in the circuit, we compute $\hat{E}_{\mathcal{B}}$, the estimate of the expectation value $\text{Tr}[\mathcal{OB}(|0\rangle\langle 0|)]$ such that

$$|\hat{E}_{\mathcal{B}} - \text{Tr}[\mathcal{OB}(|0\rangle\langle 0|)]| \leq c. \quad (7)$$

Assuming the probability of failure of the Monte Carlo algorithm to be p_{fail} , from Hoeffding's inequality we get the sampling overhead M_{EMRE} required to estimate $\text{Tr}[\mathcal{OB}(|0\rangle\langle 0|)]$ to be

$$M_{\text{EMRE}} = \frac{2}{c^2} \ln \left(\frac{2}{p_{\text{fail}}} \right), \quad (8)$$

which is a constant. This is the key result of our paper.

From the estimate $\hat{E}_{\mathcal{B}}$, we define $E_{\mathcal{B}}$, the estimate of $s\text{Tr}[\mathcal{OB}(|0\rangle\langle 0|)]$, as $E_{\mathcal{B}} := s\hat{E}_{\mathcal{B}}$. Then, by defining another quantity

$$\epsilon := cs, \quad (9)$$

we get the following bound on the estimate of $s\text{Tr}[\mathcal{OB}(|0\rangle\langle 0|)]$:

$$|E_{\mathcal{B}} - s\text{Tr}[\mathcal{OB}(|0\rangle\langle 0|)]| \leq \epsilon. \quad (10)$$

From Eq. (10), we know either of the following two equations hold.

$$0 \leq E_{\mathcal{B}} - s\text{Tr}[\mathcal{OB}(|0\rangle\langle 0|)] \leq \epsilon, \quad \text{or} \quad (11)$$

$$0 \leq s\text{Tr}[\mathcal{OB}(|0\rangle\langle 0|)] - E_{\mathcal{B}} \leq \epsilon. \quad (12)$$

By using Eq. (2), we can write

$$\text{Tr}[\mathcal{OU}(|0\rangle\langle 0|)] = s\text{Tr}[\mathcal{OB}(|0\rangle\langle 0|)] - (s-1)\text{Tr}[\mathcal{ON}(|0\rangle\langle 0|)]. \quad (13)$$

Therefore, we get the following bounds

$$E_{\mathcal{B}} - \epsilon - (s-1) \leq \text{Tr}[\mathcal{OU}(|0\rangle\langle 0|)] \leq E_{\mathcal{B}} + \epsilon + (s-1). \quad (14)$$

Since we have assumed \mathcal{O} to be a Pauli observable, it trivially holds that $|\text{Tr}[\mathcal{OU}(|0\rangle\langle 0|)]| \leq 1$. (In case \mathcal{O} is not a Pauli observable and if we denote the maximum eigenvalue of \mathcal{O} by o_{max} , then we will have $|\text{Tr}[\mathcal{OU}(|0\rangle\langle 0|)]| \leq o_{\text{max}}$.) Note that a trivial case exists when the following conditions hold:

$$2 - \epsilon - s \leq E_{\mathcal{B}} \leq \epsilon + s - 2, \quad \text{and} \quad (15)$$

$$2 \leq \epsilon + s \quad (16)$$

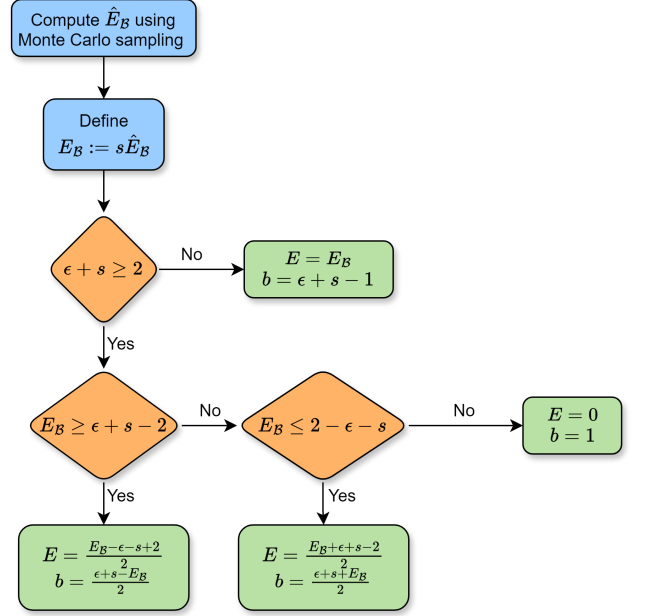


FIG. 2: Flowchart to get the final expectation value from EMRE.

In such a case, the algorithm will output the estimate E to be equal to zero and the bias b to be equal to one.

However, if one of the above three conditions in Eq. (15) and (16) are not met, we will have a non-trivial estimate and bias. To analyze the non-trivial cases, let

$$E_{\mathcal{B}} \geq \epsilon + s - 2, \quad (17)$$

then we get that $1 \leq E_{\mathcal{B}} + \epsilon + (s-1)$ and $-1 \leq E_{\mathcal{B}} - \epsilon - (s-1)$. This leads to

$$E_{\mathcal{B}} - \epsilon - (s-1) \leq \text{Tr}[\mathcal{OU}(|0\rangle\langle 0|)] \leq 1$$

from which we get the following relation

$$\left| \text{Tr}[\mathcal{OU}(|0\rangle\langle 0|)] - \frac{E_{\mathcal{B}} - \epsilon - s + 2}{2} \right| \leq \frac{\epsilon + s - E_{\mathcal{B}}}{2}. \quad (18)$$

From the above relation, we get that when Eq. (17) and (16) hold then the estimated expectation value is $(E_{\mathcal{B}} - \epsilon - s + 2)/2$ and the bias is $(\epsilon + s - E_{\mathcal{B}})/2$. We can similarly find the estimate and bias when $E_{\mathcal{B}} \leq 2 - \epsilon - s$. In this case then, the estimate would be $(E_{\mathcal{B}} + \epsilon + s - 2)/2$ and the bias would be $(\epsilon + s + E_{\mathcal{B}})/2$ which depends on $E_{\mathcal{B}}$. For the last non-trivial case when Eq. (16) is violated, i.e.,

$$\epsilon + s < 2, \quad (19)$$

will imply that $\epsilon + s - 2 \leq E_{\mathcal{B}} \leq 2 - \epsilon - s$, and the estimated expectation value is equal to $E_{\mathcal{B}}$ and the bias b is

$$b = \epsilon + s - 1 \quad (20)$$

which is a constant. A full flowchart on various cases of trivial and non-trivial instances is shown in Fig. 2.

A. Quantifying the bias in EMRE via generalized robustness

Similar to the robustness measure introduced in Ref. [32] to quantify the optimal resource cost for the probabilistic error cancellation with respect to a continuous set of implementable operations, in this subsection, we introduce the generalized robustness inspired from the generalized robustness measure defined for quantum operations in the context of dynamical resource theories [33–35]. Using this measure, we quantify the bias in EMRE. To elucidate the generalized robustness, we first give an overview of the quasi-probability distribution and the robustness below.

In the quasi-probabilistic decomposition, the idea is to decompose a quantum gate as a linear combination of the implementable gates with real coefficients such that the coefficients sum to one. By keeping together all the gates with positive coefficients and all the gates with negative coefficients, the decomposition of a unitary operation \mathcal{U} can be expressed as follows.

$$\mathcal{U} = q_+ \mathcal{B}_+ - q_- \mathcal{B}_-, \quad (21)$$

where $q_+, q_- \geq 0$, $q_+ - q_- = 1$, and \mathcal{B}_+ and \mathcal{B}_- represent quantum operations which are some convex combinations of the implementable gates. Note that such a decomposition is not unique. The PEC uses the quasi-probabilistic decomposition of all gates in the circuit to estimate the expectation value of an observable. Owing to the negative coefficients in the quasi-probabilistic decomposition, estimating the unbiased expectation value using the Monte Carlo sampling technique requires an exponential sample size. The optimal sample complexity is achieved when the quasi-probabilistic decomposition is optimal for all gates. The optimal decomposition is the decomposition with the minimum absolute sum of the coefficients in the decomposition. This minimum absolute sum of coefficients is also called the optimal overhead constant and denoted by γ in the literature [16, 32, 37]. Denoting the set of implementable operations in d -dimensions by $\mathcal{I}_{\mathcal{E}}(d)$, the optimal overhead constant, γ , can be cast as the following optimization problem

$$\gamma_{\text{opt}}(\mathcal{U}) = \min \left\{ \sum_i |b_i| \mid \mathcal{U} = \sum_i b_i \mathcal{B}_i, b_i \in \mathbb{R}, \mathcal{B}_i \in \mathcal{I}_{\mathcal{E}}(d) \right\}. \quad (22)$$

Using γ_{opt} , we can define another quantity called the robustness, $R_{\mathcal{I}_{\mathcal{E}}}$ inspired by the robustness measure in quantum resource theories. Robustness is related to the optimal overhead constant as $\gamma_{\text{opt}}(\mathcal{U}) = 2R_{\mathcal{I}_{\mathcal{E}}}(\mathcal{U}) + 1$ [32]. Using robustness, we can put a bound on the optimal overhead cost of running PEC under a given noise model.

Using the above idea of quasi-probabilistic decomposition, we now elaborate on the idea of generalized quasi-probabilistic decomposition and generalized robustness. Let a decomposition of a unitary operation \mathcal{U} be as in Eq. (21). While implementing EMRE, we approximate

the ideal \mathcal{U} in the circuit as

$$\mathcal{U} \approx q_+ \mathcal{B}_+. \quad (23)$$

If we use this approximation to find the expectation value of an observable \mathcal{O} , this translates to

$$\text{Tr}[\mathcal{O}\mathcal{U}(|0\rangle\langle 0|)] \approx q_+ \text{Tr}[\mathcal{O}\mathcal{B}_+(|0\rangle\langle 0|)], \quad (24)$$

with an (unavoidable) error of $q_- \text{Tr}[\mathcal{O}\mathcal{B}_-(|0\rangle\langle 0|)]$. However, since we are approximating the ideal gate \mathcal{U} with the positive part to evaluate the estimate of the expectation value and no longer using the negative component, it is not needed for the omitted term to be a convex combination of the implementable operations. Therefore, we can decompose \mathcal{U} as follows:

$$\mathcal{U} = s\mathcal{B} - (s-1)\mathcal{N} \quad (25)$$

with

$$\mathcal{B} = \sum_i p_i \mathcal{B}_i,$$

where $\mathcal{B}_i \in \mathcal{I}_{\mathcal{E}}(d)$ and $\mathcal{N} \in \text{CPTP}(d)$. The set $\text{CPTP}(d)$ denotes the set of all quantum channels or completely positive and trace preserving (CPTP) maps with input and output systems to be d -dimensional. By using the above decomposition, we can reduce the unavoidable error, thus getting a better estimate of the ideal expectation value.

To find the implementable operation \mathcal{B} closest to \mathcal{U} , we need to find a quantum channel \mathcal{N} that minimizes $s-1$. The optimal $s-1$ is often referred to as generalized robustness or global robustness in several resource theories [34, 36, 38–41]. In this paper, we will denote it as $R_{\mathcal{I}_{\mathcal{E}}}^+(\mathcal{U})$ and it can be cast as the following optimization problem.

$$\begin{aligned} R_{\mathcal{I}_{\mathcal{E}}}^+(\mathcal{U}) &= \min s - 1 \\ \text{s.t. } & \frac{\mathcal{U} + (s-1)\mathcal{N}}{s} \in \mathcal{I}_{\mathcal{E}}(d), \\ & s - 1 \geq 0, \mathcal{N} \in \text{CPTP}(d). \end{aligned} \quad (26)$$

The dual of the above primal problem is given by

$$\begin{aligned} R_{\mathcal{I}_{\mathcal{E}}}^+(\mathcal{U}) &= \sup \text{Tr}[J^{\mathcal{U}}\beta] - 1 \\ \text{s.t. } & 0 \leq \text{Tr}[J^Y\beta] \leq 1, \\ & \beta \geq 0, Y \in \mathcal{I}_{\mathcal{E}}(d), \end{aligned} \quad (27)$$

where $J^{\mathcal{U}}(J^Y)$ denote the Choi matrix of $\mathcal{U}(Y)$ defined as $J^{\mathcal{U}} := \text{id} \otimes \mathcal{U}(\Phi_d^+)$, and $\Phi_d^+ := \sum_{i,j} |i\rangle\langle j| \otimes |i\rangle\langle j|$ is the d -dimensional unnormalized maximally entangled state.

Furthermore, similar to the optimal overhead constant γ_{opt} defined as the absolute sum of the coefficients of the quasi-probabilistic decomposition, we define another quantity called the optimal generalized overhead constant $\gamma_{\text{opt}}^+(\mathcal{U})$ as

$$\gamma_{opt}^+(\mathcal{U}) = \min \left\{ \sum_i q_i + \sum_j n_j \left| \mathcal{U} = \sum_i q_i \mathcal{B}_i - \sum_j n_j \mathcal{N}_j, q_i, n_j \geq 0, \mathcal{B}_i \in \mathcal{I}_{\mathcal{E}}(d), \mathcal{N}_j \in \text{CPTP}(d) \right. \right\} \quad (28)$$

The optimal generalized overhead constant is related to the generalized robustness as follows $\gamma_{opt}^+(\mathcal{U}) = 2R_{\mathcal{E}}^+(\mathcal{U}) + 1$, which is similar to the relation between optimal overhead constant and robustness [32].

B. Bounds on generalized robustness

In this subsection, we derive bounds on the generalized robustness by considering specific noise models. These bounds are crucial since the bias of EMRE depends on the generalized robustness (see Eq. (20)) and therefore, by deriving bounds on generalized robustness we derive bounds on the bias in EMRE for a given noise model. This aids in analytically determining the conditions under which EMRE is effective.

We first derive a general bound on the generalized robustness given a certain decomposition of the unitary operation, while assuming an arbitrary noise acting in the circuit. Then, we derive bounds under the partially depolarizing noise, the single-qubit probabilistic noise, and the single-qubit partially dephasing noise. Under d -dimensional depolarizing noise and qubit dephasing noise, we derive an exact expression for the generalized robustness of a unitary operation. Practically, these equalities imply that to mitigate the above noise, we need not replace the ideal gate, rather we can let the error act after the ideal gate instance, and perform a post-processing in the form of multiplying the result by a factor to estimate the expectation value. Thus, these results become crucial as they save time by avoiding finding the generalized quasi-probabilistic decomposition.

Theorem 1. *Given a particular decomposition $\mathcal{U} = s\mathcal{B} - (s-1)\mathcal{N}$ where \mathcal{B} is a probabilistic combination of the implementable operations and \mathcal{N} is some quantum channel, the optimal generalized robustness is bounded by*

$$s-1 \geq R^+(\mathcal{U}) \geq \frac{1}{d^2 s} \text{Tr}[\Phi_d^+ J^{\mathcal{E}'}] \quad (29)$$

where $\mathcal{E}' = s\mathcal{B} \circ \mathcal{U}^\dagger$.

See Appendix A for the proof. Using the above theorem, we can get bounds on the generalized robustness of any unitary operation if a generalized quasi-probabilistic decomposition is known.

Theorem 2. *Consider an n -qubit unitary \mathcal{U} with local*

partially depolarizing noise $\mathcal{E}^{\text{depol}}$ of the form

$$\mathcal{E}^{\text{depol}}(\rho) = \left(1 - \frac{3p}{4}\right) \rho + \frac{p}{4} (X\rho X + Y\rho Y + Z\rho Z), \quad (30)$$

acting on each qubit after the application of \mathcal{U} . The generalized robustness of \mathcal{U} is bounded by

$$R_{\text{depol}}^+(\mathcal{U}) \leq \left(\frac{4}{4-3p}\right)^n - 1. \quad (31)$$

Furthermore, when we consider the unitary to be d -dimensional (Kraus operators can be found in [42, 43]) and the noise to be d -dimensional depolarizing noise, then we get the following exact result for the generalized robustness of \mathcal{U} :

$$R_{\text{depol}}^+(\mathcal{U}) = \frac{d^2 - 1}{d^2 + p - d^2 p}. \quad (32)$$

The proof of the above theorem is given in Appendix B. The equality in the above result, Eq. (32), implies that if the noise in the circuit is the partially depolarizing noise, then we can use the noisy circuit as it is. Mitigating the noise just involves a simple post-processing. In other words, we can obtain the mitigated expectation value by applying the noisy unitary, and multiplying the result by the factor $d^2/(d^2 + p - d^2 p)$ (for each unitary gate).

Lemma 1. *Given a single-qubit probabilistic error channel \mathcal{E} of the form*

$$\mathcal{E}(\rho) = p\mathcal{N}(\rho) + (1-p)\rho, \quad (33)$$

acting on the qubit after the application of a single-qubit operation \mathcal{U} , the generalized robustness of \mathcal{U} is bounded by

$$R^+(\mathcal{U}) \leq \left(\frac{p}{1-p}\right) \quad (34)$$

Theorem 3. *Given the single-qubit dephasing error $\mathcal{E}^{\text{deph}}$ of the form*

$$\mathcal{E}^{\text{deph}}(\rho) = \left(1 - \frac{p}{2}\right) \rho + \frac{p}{2} (Z\rho Z), \quad (35)$$

acting on the qubit after the application of a single-qubit operation \mathcal{U} , the generalized robustness of \mathcal{U} is equal to

$$R_{\text{deph}}^+(\mathcal{U}) = \frac{p}{2-p}. \quad (36)$$

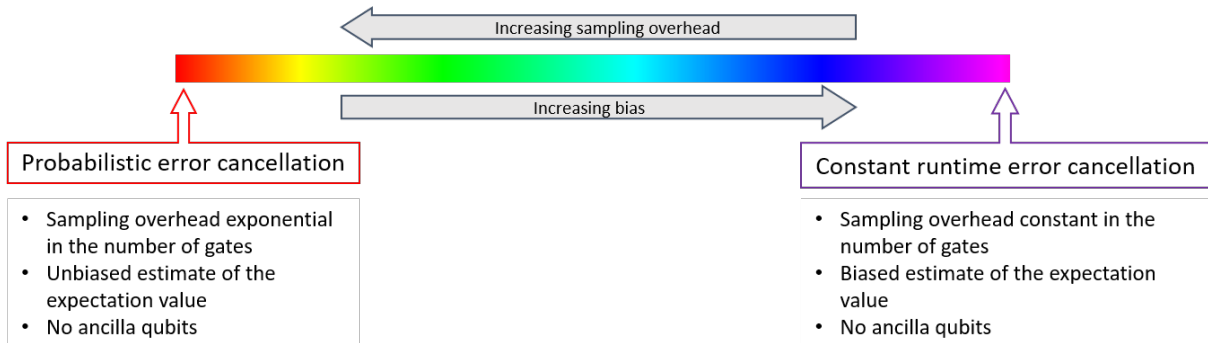


FIG. 3: Family of error mitigation protocols color coded in the spectrum where PEC sits at one end and EMRE at the other end. Everything in between is HEMRE.

The proofs of Lemma 1 and Theorem 3 are provided in Appendix C. It is interesting to note that while it is challenging to find the quasi-probabilistic decomposition to perform PEC for a given error, the problem becomes slightly less challenging (and time-saving) if we are applying EMRE when the errors can be expressed as local and probabilistic quantum operations. The reason for this is that we can get the decomposition for EMRE for the probabilistic noise from the very definition of the noise, thus saving us time in finding the decomposition. In such a case of probabilistic noise, we also theoretically know the upper bound on the generalized robustness using which we can estimate the sampling size for EMRE. Further, if the noise is a single-qubit dephasing noise, we can let the desired unitary channel be in the circuit as it is, similar to the case of d -dimensional depolarizing noise. To mitigate noise in such a specific case, we only need to multiply the estimate of the expectation value by a factor that depends on the probability of noise.

IV. HYBRID ERROR MITIGATION BY RESTRICTED EVOLUTION (HEMRE)

EMRE estimates the expectation value of an observable using only a constant sampling overhead and is very reliable for quantum gates with low noise probability of the current quantum hardware [44–47]. However, for noisy hardware with higher noise probabilities, bias from the EMRE’s expectation value increases. To tackle this problem along with an intention to suppress the sampling overhead required by PEC, we develop a hybrid approach by combining EMRE and PEC, resulting in the hybrid error mitigation by restricted evolution (HEMRE) with better sampling overhead than the PEC and better bias than the EMRE.

There are two ways to construct such a hybrid algorithm. In the first approach, the strategy is to reduce the sampling overhead given a desired minimum precision in estimating the result. In this approach, the maximum allowed bias can be treated as a parameter, and we can view EMRE, HEMRE, and PEC together on a spectrum

as shown in Fig. 3 where EMRE and PEC lie on the extreme ends. In the second approach, the strategy is to minimize the bias given a fixed sampling overhead. This is achieved by using the Hoeffding inequality that provides a connection between the sampling overhead and the bias. Below, we provide the details of the algorithm of the former approach. The algorithm for the latter case can be constructed in a similar fashion. Importantly, for both strategies, one must know in advance both a quasi-probabilistic and a generalized quasi-probabilistic decomposition of each unitary gate \mathcal{U}_i present in the circuit. Trivially, the best result is obtained when the decompositions are optimal.

Let us look at HEMRE in full glory and how one can combine EMRE and PEC, given a maximum tolerable bias to reduce the sampling overhead. The question at hand is which gates in the circuit need to be approximated to the closest implementable gates such that the bias in the result does not exceed Δ_{fixed} , the allowed fixed bias for estimating the expectation value. In the previous section/discussion on EMRE, we found that the bias depends on the generalized robustness of the gates in the circuit. We take advantage of this information to answer the above question for HEMRE. In other words, we need to put a constraint on the product of the generalized robustness of the gates that will be approximated. Using this constraint, we can find those gates which obey the constraint and we can approximate them to their closest implementable gates or a convex combination thereof.

Gate	Frequency	Gen. robustness	Total gen. robustness
\mathcal{G}_1	n_1	s_1	$(s_1)^{n_1}$
\mathcal{G}_2	n_2	s_2	$(s_2)^{n_2}$
\mathcal{G}_3	n_3	s_3	$(s_3)^{n_3}$
\mathcal{G}_4	n_4	s_4	$(s_4)^{n_4}$

TABLE I: Information required for selecting gates to be approximated for HEMRE

We denote s to be the product of the generalized robustness of all gates in the circuits as defined in Eq. (3) and

γ to be the product of the robustness of all gates in the circuit. From Eq. (8), (9) and discussions in Ref. [16], the sampling overhead is proportional to the square of the product of the robustness or the generalized robustness of the gates in the circuit. The key idea here is that we selectively choose to keep the quasi-probabilistic decomposition of some gates and for the remaining others, we approximate them with the implementable gates as obtained from their generalized quasi-probability decomposition. Of course, this selection depends on the input Δ_{fixed} that a user desires. By using the Monte-Carlo sampling technique to estimate the expectation value upto ϵ ($= cs$) precision and with success probability $1 - p_{\text{fail}}$, the sampling overhead M_{HEMRE} is found to be

$$M_{\text{HEMRE}} = \frac{2s_{\text{incl}}^2 \gamma_{\text{incl}}^2}{(cs)^2} \ln \left(\frac{2}{p_{\text{fail}}} \right), \quad (37)$$

where γ_{incl} is the product of the robustness of the gates whose quasi-probability decomposition are chosen for the HEMRE, and s_{incl} is the product of the generalized robustness of the gates whose generalized quasi-probability decomposition are chosen. The bias Δ or the deviation from the actual expectation value can be calculated in a similar way as in EMRE, by considering s_{incl} instead of s . As seen in the EMRE, the bias for the case when $\epsilon + s_{\text{incl}} \geq 2$ depends on $E_{\mathcal{B}}$. Since we first need to choose the gates that are going to be approximated, we need to consider only the case where $\epsilon + s_{\text{incl}} < 2$ to put a constraint on s_{incl} . Additionally, we need to take into account the fact that the bias is $\epsilon + s_{\text{incl}} - 1$ and we need this value not to be more than the user's input, Δ_{fixed} . Therefore, we get the following constraint on the product of the generalized robustness, s_{incl} , of the approximated gates to be

$$s_{\text{incl}} \leq \Delta_{\text{fixed}} + 1 - \epsilon. \quad (38)$$

Using this constraint, we can choose which gates to be approximated. For the remaining gates, we will use their full quasi-probabilistic decomposition. There are several ways to realize this strategy. We have listed a number of them in the Appendix D. Below, we provide the details of one such method which maximizes the number of gates to be approximated.

To maximize the number of gates to be approximated to the closest (convex combination of) implementable gate(s) for HEMRE, we first need to identify the unique gates in the circuit and compute their generalized robustness. Using this information, we can construct a table similar to Table I. We can then sort the table according to the generalized robustness such that $s_1 \leq s_2 \leq s_3 \leq \dots$. Using this sorted table, we can easily find which gates and how many of those gates are required such that the product of their generalized robustness meet the criterion in Eq. (38). We also provide an algorithm (see Algorithm 1) to select the maximum number of gates to be approximated such that approximating one more extra gate will violate the constraint of Eq. (38). For the remainder of

Algorithm1 An algorithm to approximate maximum number of gates for HEMRE

Input: i. Maximum tolerable bias, Δ_{fixed} ,
ii. Gates' information (as in Table I) sorted in increasing order of the generalized robustness.

Pre-computation:

- i. Create a frequency dictionary, say $fr = \{\text{gate} : \text{frequency}\}$, containing the frequency of occurrence of corresponding gates in the circuit.
- ii. Create another dictionary, $gr = \{\text{gate} : \text{generalized robustness}\}$, containing the generalized robustness of corresponding gates.

Output: All the gates that need to be replaced, and the corresponding total s_{incl} .

```

1:  $s_{\text{incl}} \leftarrow 1$ 
2: for gate in unique_gates do
3:   if  $s_{\text{incl}} * (gr[\text{gate}])^{fr[\text{gate}]} \leq \Delta_{\text{fixed}} - \epsilon + 1$  then
4:      $s_{\text{incl}} \leftarrow s_{\text{incl}} * (gr[\text{gate}])^{fr[\text{gate}]}$ 
5:     Approximate all occurrences of 'gate' in the circuit
6:   else
7:      $m = \left\lfloor \log \left( \frac{\Delta_{\text{fixed}} - \epsilon + 1}{s_{\text{incl}}} \right) / \log (gr[\text{gate}]) \right\rfloor$ 
8:      $s_{\text{incl}} \leftarrow s_{\text{incl}} * (gr[\text{gate}])^m$ 
9:     Approximate  $m$  occurrences of 'gate' in the circuit
10:  Return

```

the gates, we consider their quasi-probabilistic decomposition.

The reason for taking this approach of first restricting gates with the smallest generalized robustness over other approaches is that this way we are not losing much information per approximated gate. This happens because, for the gate with lesser generalized robustness, the ratio between the norm of the positive and the negative part norm will be bigger as compared to that of a gate with larger generalized robustness. In other words, this implies that for the gate with smaller generalized robustness, the quantum operation that we get by normalizing the positive part of the gate's decomposition is closer to the original gate (in diamond norm) as compared to the quantum operation that we get by normalizing the positive part of the gate with higher generalized robustness. Thus, when we restrict a gate with a larger generalized robustness (to its positive part), the approximation is not too close to the original gate and thus, it is better to restrict the gates with a smaller generalized robustness.

V. NUMERICAL ANALYSES

In this section, we present the numerical analyses of our error mitigation protocols: EMRE and HEMRE. We benchmark our protocols against the state-of-the-art, probabilistic error cancellation and find that EMRE and HEMRE perform better than PEC. We conduct the numerical analyses by considering two practically significant noise models: the partially depolarizing noise and the inhomogeneous Pauli noise model. We present the results of the depolarizing noise in this section and the

results of the inhomogeneous Pauli noise are presented in Appendix E.

For the numerical analyses, we use the SWAP-test to test how much the $|000\rangle$ state differs from the $|GHZ\rangle$ state. The ideal value of this test for the given states is 0.5. We model the noisy circuit by appending the noisy channel after each gate instance in the circuit. We then deploy the error mitigation protocols and estimate how much the two states differ from each other. The difference of the obtained value from 0.5 is the bias and we analyze how the bias changes as the noise probability changes for different mitigation protocols.

To implement the SWAP-test, we use the C-SWAP circuit composed of T , T^\dagger , Hadamard, and controlled-NOT gates (see Fig. 4 Sec. XI of Ref. [17] for the circuit). The circuit consists of 7 qubits and 140 gates. We assume the depolarization noise to be acting locally after every gate. By simulating such a noisy circuit, we then numerically compute the expectation value of $\langle Z \rangle$ on the first qubit of the C-SWAP circuit which quantifies how much the two input states differ. We obtain the estimate of the expectation value for different depolarizing noise probabilities. For each noise probability, we estimate the expectation values for five cases – first, by using no error mitigation, second, by deploying PEC with 1,000 samplings, third,

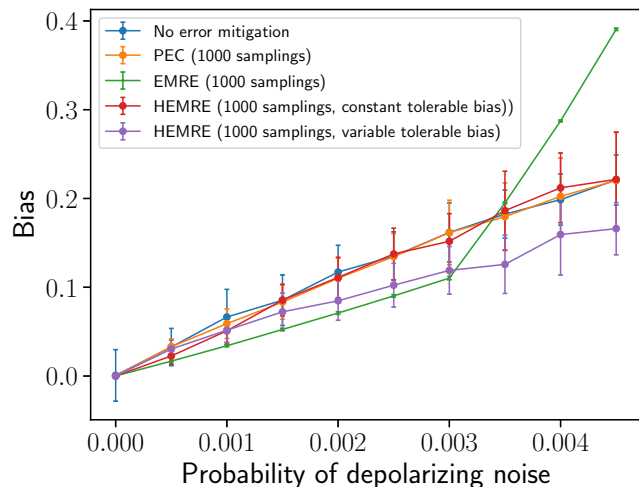


FIG. 4: Comparison of the performance of EMRE and HEMRE against PEC and no EM under the partially depolarizing noise. In this comparison, we have considered two cases for HEMRE: one, where we fix the tolerable bias to be 0.05 for all noise probabilities, and the other, where we increase the tolerable bias as the noise probability increases. In the latter case, the tolerable bias is chosen to be the mean bias we get from PEC. We see from the above figure that EMRE outperforms PEC and HEMRE up to a certain noise probability, beyond which HEMRE (with variable tolerable bias) continues to consistently perform better than PEC.

by deploying EMRE with 1,000 samplings, fourth, by deploying HEMRE with 1,000 samplings and by fixing the tolerable bias to be 0.05 for all noise probabilities, and lastly, by deploying HEMRE with 1,000 samplings and increasing the tolerable bias with the increasing noise probability. In the last case, we choose the tolerable bias for each noise probability to be the mean bias from the PEC’s numerical results for the same noise probability.

The results are shown in Fig. 4. For each depolarizing noise probability, we obtained 50 estimates for each of the five cases mentioned above. From these 50 estimates, we obtained the mean bias and the standard deviation, and then we plotted the mean bias against the depolarizing noise probability which is shown in the figure. Moreover, for estimating each expectation value, we use the same number of samplings across different EM techniques to make a fair comparison in the bias. PEC will give a zero bias if the number of samplings is increased. However, the sampling overhead for PEC increases exponentially with respect to the noise probability making it practically impossible to run with such high sampling overhead for higher noise probabilities. Therefore, PEC is often deployed with fewer number of samples. For EMRE, we need to fix a constant ‘c’ which gives us the constant sampling overhead. Here, we did the reverse by fixing the sampling overhead and obtained ‘c’ which just impacts the precision of estimating $E_{\mathcal{B}}$ in Eq. 10. So, the more the number of samples, the better we estimate $E_{\mathcal{B}}$. However, the bias isn’t impacted much as is apparent from the standard deviation in EMRE’s results in Fig. 4 (or the spread of the EMRE distributions in Fig. 5, 8, or 9). For HEMRE, the number of samples needed depends on the tolerable bias based on which the protocol decides which gates to approximate and for which gates the full decomposition needs to be used. In the current analyses, since we fixed the number of samples, we see that in the first case of HEMRE where we fixed the tolerable bias, HEMRE performs similar to PEC as expected. In the case where we increase the tolerable bias for HEMRE with increasing probability, the mean bias that we obtained from HEMRE consistently remained better than that of PEC.

From the analyses, we see that for the given circuit and noise probabilities below 0.003 (that is, gate fidelities to be around 99.7% and more), EMRE outperforms HEMRE and PEC. For these probabilities, we found the bias from EMRE to be about 40% better than that of PEC. Another key observation we make from the figure is that the error bars from the EMRE are very small as compared to the rests, noticing that the estimates from EMRE are stable across samplings. In other words, EMRE demonstrates superior sample efficiency compared to PEC, particularly for low noise probabilities. While PEC exhibits significant bias and uncertainty for reduced sample size, EMRE consistently yields accurate estimates of the ideal expectation value with significantly fewer samples. For larger noise probabilities, where the bias from EMRE starts to diverge due to the

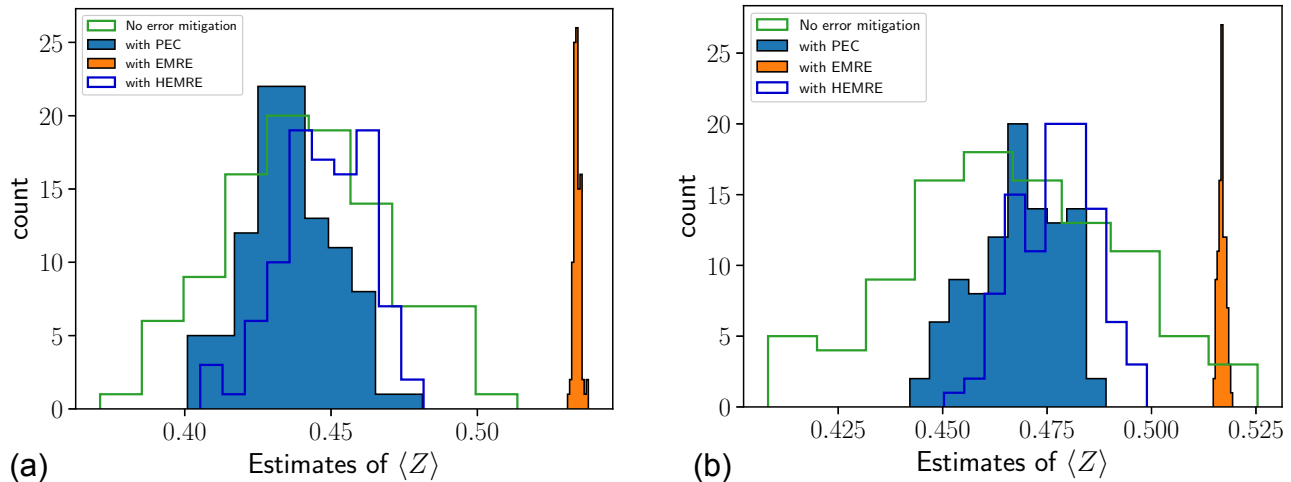


FIG. 5: Plots of the distribution of the 100 estimates of the expectation value of Z obtained without any error mitigation, with PEC, with EMRE, and with HEMRE by considering (a) depolarizing noise probability of 0.001 and (b) depolarizing noise probability of 0.0005. When PEC, EMRE, or HEMRE were deployed for mitigating errors, 1000 samplings were taken to obtain each $\langle Z \rangle$ estimate in the controlled-SWAP circuit. In the above plots, the tolerable bias for HEMRE was kept fixed to be 0.05.

growing generalized robustness of the gates, we can rely on HEMRE. We see from the figure that as the noise probability increases, the HEMRE (for which the tolerable noise varied with the noise probability) consistently gave a lower bias than PEC while utilizing the same number of samples. This was expected since HEMRE acquires properties of both EMRE and PEC, and approximates fewer gates (thus saving runtime or sampling overhead) based on the maximum tolerable bias provided.

Further, in Fig. 5(a) and Fig. 5(b), we provide the distribution of the 100 expectation value estimates for the case of no EM, PEC, EMRE, and HEMRE with 0.05 tolerable bias, for noise probabilities 0.001 and 0.0005, respectively. We see that in both Fig. 5(a) and 5(b), the largest spread of the estimates is from the case when no error mitigation is deployed indicating that the result with no EM cannot be trusted. When PEC is deployed, we see that the variance of the distribution becomes smaller. However, since we only used 1000 samples, we do not get zero bias. For EMRE, we find that the variance is very small indicating the reliability of the estimate. However, unlike PEC, increasing the sampling size will not decrease the bias in the result. The key difference between EMRE and PEC is that when we have a constraint on the sampling size, EMRE's results have more reliability and will have a smaller bias on average as compared to PEC. Lastly, we see that for HEMRE, the distribution is shifted towards the ideal value, however, the variance is almost similar to that of PEC's distribution. The reason is the same as that of PEC which is less number of sample size, although some gates were approximated by HEMRE as the tolerable bias was fixed to 0.05, making the distribution shift towards the ideal value.

In Fig. 6 (Appendix), we also present the histograms for the measured expectation values and the unbiased estimates obtained when using PEC, EMRE, and HEMRE, under depolarizing noise. Taking the average of the unbiased estimates gives us the estimate of the expectation value. We see that for each circuit run, both PEC and EMRE span almost the same set of expectation values. The main difference arises in the unbiased expectation values where we need to multiply the measured expectation values with the norm and the respective sign as obtained from the decomposition.

In the end, we'd like to remark that for the numerical demonstrations here, we have used the quasi-probabilistic decomposition used in PEC and restricted it to its positive part to perform EMRE. Executing EMRE by restricting the quasi-probability distribution however, is not the most optimal way as we have shown in Section III, and using the optimal EMRE decomposition will give us even better bias.

VI. DISCUSSION

We introduce two new error mitigation protocols, namely error mitigation by restricted evolution (EMRE) and hybrid EMRE (HEMRE). EMRE offers a constant sampling overhead at the cost of a biased estimate of the expectation value. HEMRE, on the other hand, takes the maximum allowed bias from the user, and then selectively approximates some gates in the circuit, and outputs the estimate of the expectation value with runtime smaller than that of PEC, and bias less than or equal to the maximum tolerable bias. We establish that the bias in EMRE is dependent on a measure called generalized

robustness, and derive bounds on it under different practically significant noise models, thus finding bounds on the EMRE’s biases. We numerically demonstrate that for low noise probabilities that we have from current quantum hardware, EMRE produces a better estimate of expectation value compared to PEC with limited samples. This is particularly relevant as we are gradually advancing to the era of early fault-tolerant quantum computing where one would combine some error correction with error mitigation techniques to perform more reliable quantum computation [48, 49]. As the field is progressing, various companies and research groups working on quantum hardware are claiming to reduce the logical error rate within the next five years to as low as 10^{-6} by 2025-26 [50]. In such cases, EMRE is more reliable than PEC as it requires much less sampling overhead and gives a better bias.

The efficacy of combining gate set tomography, as employed in [17], with our proposed techniques for mitigating localized and non-Markovian errors in quantum computers remains an open question. Additionally, the impact of this integration on algorithmic runtime requires further investigation. A promising avenue for future research is the dynamic application of EMRE or HEMRE. By continuously approximating gates based on observed

errors, we seek to predict and mitigate subsequent errors more effectively. Reinforcement learning or deep learning approaches may prove instrumental in achieving this goal. The synergy between EMRE or HEMRE and error correction holds significant potential for advancing the early fault-tolerant quantum computing era. By exploring novel error mitigation protocols that circumvent the exponential scaling of existing methods, we believe our proposals aim to accelerate progress in the field.

ACKNOWLEDGMENTS

We would like to thank Zhenyu Cai, Abhinav Kandala, Ying Li and Zlatko Mineev, for helpful discussions. We would also like to thank the anonymous referees of AQIS 2024 for their comments which helped us to polish certain aspects of the paper. Lastly, we thank our management executives- Kevin Ferreira, Yipeng Ji, Paria Nejat of LG Electronics Toronto AI Lab for their constant support throughout this work. Last but not least, we are grateful to Euwern Teh of LG Electronics Toronto AI Lab for showing us how to draw beautiful quantum circuits. Throughout our numerical computations, we used the open-source software Mitiq [51] to deploy PEC in circuits.

-
- [1] Torsten Hoefler, Thomas Häner, and Matthias Troyer, “Disentangling Hype from Practicality: On Realistically Achieving Quantum Advantage,” *Commun. ACM* **66**, 82–87 (2023).
- [2] Joonho Lee, Dominic W. Berry, Craig Gidney, William J. Huggins, Jarrod R. McClean, Nathan Wiebe, and Ryan Babbush, “Even More Efficient Quantum Computations of Chemistry Through Tensor Hypercontraction,” *PRX Quantum* **2**, 030305 (2021).
- [3] Andrew J. Daley, Immanuel Bloch, Christian Kokail, Stuart Flannigan, Natalie Pearson, Matthias Troyer, and Peter Zoller, “Practical quantum advantage in quantum simulation,” *Nature* **607**, 667–676 (2022).
- [4] Xiangyu Li, Xiaolong Yin, Nathan Wiebe, Jaehun Chun, Gregory K. Schenter, Margaret S. Cheung, and Johannes Mühlmenstädt, “Potential quantum advantage for simulation of fluid dynamics,” *arXiv* (2023), 10.48550/arXiv.2303.16550, 2303.16550.
- [5] Kishor Bharti, Alba Cervera-Lierta, Thi Ha Kyaw, Tobias Haug, Sumner Alperin-Lea, Abhinav Anand, Matthias Degroote, Hermann Heimonen, Jakob S. Kottmann, Tim Menke, *et al.*, “Noisy intermediate-scale quantum algorithms,” *Rev. Mod. Phys.* **94**, 015004 (2022).
- [6] Jules Tilly, Hongxiang Chen, Shuxiang Cao, Dario Picozzi, Kanav Setia, Ying Li, Edward Grant, Leonard Wossnig, Ivan Rungger, George H. Booth, *et al.*, “The Variational Quantum Eigensolver: A review of methods and best practices,” *Phys. Rep.* **986**, 1–128 (2022).
- [7] M. Cerezo, Andrew Arrasmith, Ryan Babbush, Simon C. Benjamin, Suguru Endo, Keisuke Fujii, Jarrod R. McClean, Kosuke Mitarai, Xiao Yuan, Lukasz Cincio, and Patrick J. Coles, “Variational quantum algorithms,” *Nat. Rev. Phys.* **3**, 625–644 (2021).
- [8] Edward Farhi, Jeffrey Goldstone, and Sam Gutmann, “A Quantum Approximate Optimization Algorithm,” *arXiv* (2014), 10.48550/arXiv.1411.4028, 1411.4028.
- [9] Alberto Peruzzo, Jarrod McClean, Peter Shadbolt, Man-Hong Yung, Xiao-Qi Zhou, Peter J. Love, Alán Aspuru-Guzik, and Jeremy L. O’Brien, “A variational eigenvalue solver on a photonic quantum processor,” *Nat. Commun.* **5**, 1–7 (2014).
- [10] Dave Wecker, Matthew B. Hastings, and Matthias Troyer, “Progress towards practical quantum variational algorithms,” *Phys. Rev. A* **92**, 042303 (2015).
- [11] Jarrod R. McClean, Jonathan Romero, Ryan Babbush, and Alán Aspuru-Guzik, “The theory of variational hybrid quantum-classical algorithms,” *New J. Phys.* **18**, 023023 (2016).
- [12] Thi Ha Kyaw, Micheline B. Soley, Brandon Allen, Paul Bergold, Chong Sun, Victor S. Batista, and Alán Aspuru-Guzik, “Boosting quantum amplitude exponentially in variational quantum algorithms,” *Quantum Sci. Technol.* **9**, 01LT01 (2023).
- [13] Sergey Bravyi, David Gosset, and Ramis Movassagh, “Classical algorithms for quantum mean values,” *Nat. Phys.* **17**, 337–341 (2021).
- [14] Gaurav Saxena, Ahmed Shalabi, and Thi Ha Kyaw, “Practical limitations of quantum data propagation on noisy quantum processors,” *Phys. Rev. Appl.* **21**, 054014 (2024).

- [15] Ying Li and Simon C. Benjamin, “Efficient Variational Quantum Simulator Incorporating Active Error Minimization,” *Phys. Rev. X* **7**, 021050 (2017).
- [16] Kristan Temme, Sergey Bravyi, and Jay M. Gambetta, “Error miti for Short-Depth Quantum Circuits,” *Phys. Rev. Lett.* **119**, 180509 (2017).
- [17] Suguru Endo, Simon C. Benjamin, and Ying Li, “Practical Quantum Error Mitigation for Near-Future Applications,” *Phys. Rev. X* **8**, 031027 (2018).
- [18] X. Bonet-Monroig, R. Sagastizabal, M. Singh, and T. E. O’Brien, “Low-cost error mitigation by symmetry verification,” *Phys. Rev. A* **98**, 062339 (2018).
- [19] Tudor Giurgica-Tiron, Yousef Hindy, Ryan LaRose, Andrea Mari, and William J. Zeng, “Digital zero noise extrapolation for quantum error mitigation,” in *2020 IEEE International Conference on Quantum Computing and Engineering (QCE)* (IEEE, 2020) pp. 306–316.
- [20] Jinzhao Sun, Xiao Yuan, Takahiro Tsunoda, Vlatko Vedral, Simon C. Benjamin, and Suguru Endo, “Mitigating Realistic Noise in Practical Noisy Intermediate-Scale Quantum Devices,” *Phys. Rev. Appl.* **15**, 034026 (2021).
- [21] Andrew Shaw, “Classical-Quantum Noise Mitigation for NISQ Hardware,” *arXiv* (2021), 10.48550/arXiv.2105.08701, 2105.08701.
- [22] Angus Lowe, Max Hunter Gordon, Piotr Czarnik, Andrew Arrasmith, Patrick J. Coles, and Lukasz Cincio, “Unified approach to data-driven quantum error mitigation,” *Phys. Rev. Res.* **3**, 033098 (2021).
- [23] Bálint Koczor, “Exponential Error Suppression for Near-Term Quantum Devices,” *Phys. Rev. X* **11**, 031057 (2021).
- [24] Kun Wang, Yuanyi Chen, and Xin Wang, “Mitigating quantum errors via truncated neumann series,” *Science China Information Sciences* **66** (2021).
- [25] Yasunari Suzuki, Suguru Endo, Keisuke Fujii, and Yuuki Tokunaga, “Quantum Error Mitigation as a Universal Error Reduction Technique: Applications from the NISQ to the Fault-Tolerant Quantum Computing Eras,” *PRX Quantum* **3**, 010345 (2022).
- [26] Daniel Bultrini, Max Hunter Gordon, Piotr Czarnik, Andrew Arrasmith, M. Cerezo, Patrick J. Coles, and Lukasz Cincio, “Unifying and benchmarking state-of-the-art quantum error mitigation techniques,” *Quantum* **7**, 1034 (2023), 2107.13470v2.
- [27] Zhenhuan Liu, Xingjian Zhang, Yue-Yang Fei, and Zhenyu Cai, “Virtual channel purification,” (2024), *arXiv:2402.07866 [quant-ph]*.
- [28] Youngseok Kim, Andrew Eddins, Sajant Anand, Ken Xuan Wei, Ewout van den Berg, Sami Rosenblatt, Hasan Nayfeh, Yantao Wu, Michael Zaletel, Kristan Temme, and Abhinav Kandala, “Evidence for the utility of quantum computing before fault tolerance,” *Nature* **618**, 500–505 (2023).
- [29] Zhenyu Cai, Ryan Babbush, Simon C. Benjamin, Suguru Endo, William J. Huggins, Ying Li, Jarrod R. McClean, and Thomas E. O’Brien, “Quantum error mitigation,” *Rev. Mod. Phys.* **95**, 045005 (2023).
- [30] Ryuji Takagi, Suguru Endo, Shintaro Minagawa, and Mile Gu, “Fundamental limits of quantum error mitigation,” *npj Quantum Inf.* **8**, 1–11 (2022).
- [31] Yihui Quek, Daniel Stilck França, Sumeet Khatri, Johannes Jakob Meyer, and Jens Eisert, “Exponentially tighter bounds on limitations of quantum error mitigation,” *Nat. Phys.*, 1–11 (2024).
- [32] Ryuji Takagi, “Optimal resource cost for error mitigation,” *Phys. Rev. Res.* **3**, 033178 (2021).
- [33] Yunchao Liu and Xiao Yuan, “Operational resource theory of quantum channels,” *Phys. Rev. Res.* **2**, 012035 (2020).
- [34] Zi-Wen Liu and Andreas Winter, “Resource theories of quantum channels and the universal role of resource erasure,” *arXiv* (2019), 10.48550/arXiv.1904.04201, 1904.04201.
- [35] Gaurav Saxena, Eric Chitambar, and Gilad Gour, “Dynamical resource theory of quantum coherence,” *Phys. Rev. Res.* **2**, 023298 (2020).
- [36] Gaurav Saxena and Gilad Gour, “Quantifying multiqubit magic channels with completely stabilizer-preserving operations,” *Phys. Rev. A* **106**, 042422 (2022).
- [37] Ewout van den Berg, Zlatko K. Mineev, Abhinav Kandala, and Kristan Temme, “Probabilistic error cancellation with sparse Pauli-Lindblad models on noisy quantum processors,” *Nat. Phys.* **19**, 1116–1121 (2023).
- [38] James R. Seddon, Bartosz Regula, Hakop Pashayan, Yingkai Ouyang, and Earl T. Campbell, “Quantifying quantum speedups: Improved classical simulation from tighter magic monotones,” *PRX Quantum* **2**, 010345 (2021).
- [39] Fernando G. S. L. Brandão and Gilad Gour, “Reversible framework for quantum resource theories,” *Phys. Rev. Lett.* **115**, 070503 (2015).
- [40] Eric Chitambar and Gilad Gour, “Quantum resource theories,” *Rev. Mod. Phys.* **91**, 025001 (2019).
- [41] Ryuji Takagi and Bartosz Regula, “General resource theories in quantum mechanics and beyond: Operational characterization via discrimination tasks,” *Phys. Rev. X* **9**, 031053 (2019).
- [42] Poolad Imany, Jose A. Jaramillo-Villegas, Mohammed S. Alshaykh, Joseph M. Lukens, Ogaga D. Odele, Alexandria J. Moore, Daniel E. Leaird, Minghao Qi, and Andrew M. Weiner, “High-dimensional optical quantum logic in large operational spaces,” *npj Quantum Inf.* **5**, 1–10 (2019).
- [43] Pranav Gokhale, Jonathan M. Baker, Casey Duckering, Natalie C. Brown, Kenneth R. Brown, and Frederic T. Chong, “Asymptotic improvements to quantum circuits via qutrits,” in *ISCA ’19: Proceedings of the 46th International Symposium on Computer Architecture* (Association for Computing Machinery, New York, NY, USA, 2019) pp. 554–566.
- [44] Riddhi S. Gupta, Neereja Sundaresan, Thomas Alexander, Christopher J. Wood, Seth T. Merkel, Michael B. Healy, Marius Hillenbrand, Tomas Jochym-O’Connor, James R. Wootton, Theodore J. Yoder, Andrew W. Cross, Maika Takita, and Benjamin J. Brown, “Encoding a magic state with beyond break-even fidelity,” *Nature* **625**, 259–263 (2024).
- [45] Dolev Bluvstein, Simon J. Evered, Alexandra A. Geim, Sophie H. Li, Hengyun Zhou, Tom Manovitz, Sepehr Ebadi, Madelyn Cain, Marcin Kalinowski, Dominik Hangleiter, J. Pablo Bonilla Ataides, Nishad Maskara, Iris Cong, Xun Gao, Pedro Sales Rodriguez, Thomas Karolyshyn, Giulia Semeghini, Michael J. Gullans, Markus Greiner, Vladan Vuletić, and Mikhail D. Lukin, “Logical quantum processor based on reconfigurable atom arrays,” *Nature* **626**, 58–65 (2024).
- [46] Leonid Abdurakhimov, Janos Adam, Hasnain Ahmad, Olli Ahonen, Manuel Algaba, Guillermo Alonso,

- Ville Bergholm, Rohit Beriwal, Matthias Beuerle, Clinton Bockstiegel, Alessio Calzona, Chun Fai Chan, Daniele Cucurachi, Saga Dahl, Rakhim Davletkaliyev, *et al.*, “Technology and Performance Benchmarks of IQM’s 20-Qubit Quantum Computer,” [arXiv \(2024\)](#), [10.48550/arXiv.2408.12433](#), [2408.12433](#).
- [47] Rajeev Acharya, Laleh Aghababaie-Beni, Igor Aleiner, Trond I. Andersen, Markus Ansmann, Frank Arute, Kunal Arya, Abraham Asfaw, Nikita Astrakhantsev, Juan Atalaya, Ryan Babbush, Dave Bacon, Brian Ballard, Joseph C. Bardin, Johannes Bausch, *et al.*, “Quantum error correction below the surface code threshold,” [arXiv \(2024\)](#), [10.48550/arXiv.2408.13687](#), [2408.13687](#).
- [48] William J. Huggins, Sam McArdle, Thomas E. O’Brien, Joonho Lee, Nicholas C. Rubin, Sergio Boixo, K. Birgitta Whaley, Ryan Babbush, and Jarrod R. McClean, “Virtual Distillation for Quantum Error Mitigation,” [Phys. Rev. X **11**, 041036 \(2021\)](#).
- [49] Alvin Gonzales, Anjala M. Babu, Ji Liu, Zain Saleem, and Mark Byrd, “Fault Tolerant Quantum Error Mitigation,” [arXiv \(2023\)](#), [10.48550/arXiv.2308.05403](#), [2308.05403](#).
- [50] “Our quantum computing journey – Google Quantum AI,” (2021), [Online; accessed 4. Sep. 2024].
- [51] Ryan LaRose, Andrea Mari, Sarah Kaiser, Peter J. Karalekas, Andre A. Alves, Piotr Czarnik, Mohamed El Mandouh, Max H. Gordon, Yousef Hindy, Aaron Robertson, Purva Thakre, Misty Wahl, Danny Samuel, Rahul Mistry, Maxime Tremblay, Nick Gardner, Nathaniel T. Stemen, Nathan Shammah, and William J. Zeng, “Mitiq: A software package for error mitigation on noisy quantum computers,” [Quantum **6**, 774 \(2022\)](#).

Appendix A: Proof of Theorem 1

Theorem 1 statement. Given a particular decomposition $\mathcal{U} = s\mathcal{B} - (s-1)\mathcal{N}$ where \mathcal{B} is a probabilistic combination of the implementable operations and \mathcal{N} is some quantum channel, the optimal generalized robustness is bounded by

$$s - 1 \geq R^+(\mathcal{U}) \geq \frac{1}{d^2 s} \text{Tr}[\Phi_d^+ J^{\mathcal{E}'}] \quad (\text{A1})$$

where $\mathcal{E}' = s\mathcal{B} \circ \mathcal{U}^\dagger$.

Proof. The upper bound of the above theorem follows from the primal form of the optimization problem of the generalized robustness given in Eq. 26.

For the lower bound, let \mathcal{E} be the error acting after every gate and let a decomposition of \mathcal{U} be $\mathcal{U} = \sum_i v_i \mathcal{E} \circ \mathcal{V}_i - n\mathcal{N}$ where $v_i, n \geq 0$. We can rearrange this as

$$\mathcal{U} + n\mathcal{N} = \mathcal{E} \circ \left(\sum_i v_i \mathcal{V}_i \right) \quad (\text{A2})$$

Let us define another channel $\mathcal{E}' := \sum_i v_i \mathcal{V}_i \circ \mathcal{U}^\dagger$. Then the following holds

$$\mathcal{E} \circ \mathcal{E}' = \text{id} + n\mathcal{N} \circ \mathcal{U}^\dagger \geq \text{id} \quad (\text{A3})$$

where id denotes the identity channel. Then following the arguments of Appendix C of [32], $\mathcal{E}' \circ \mathcal{E} \geq \text{id}$ will also hold as long as $\mathcal{V}_i, \mathcal{E} \in \text{CPTP}(d)$. Now let

$$\beta := \frac{J^{\mathcal{E}' \circ \mathcal{U}}}{d^2 (\sum_i v_i)} \geq 0.$$

Then for any $\mathcal{W} \in \text{CPTP}(d)$, we get

$$\text{Tr}[J^{\mathcal{E} \circ \mathcal{W}} \beta] = \frac{1}{d^2 \sum_i v_i} \text{Tr}[J^{\mathcal{E} \circ \mathcal{W}} J^{\mathcal{E}' \circ \mathcal{U}}] \quad (\text{A4})$$

$$= \frac{1}{\sum_i v_i} \text{Tr} \left[\left(\text{id} \otimes \mathcal{E}' \circ \mathcal{E} \left(\frac{J^{\mathcal{W}}}{d} \right) \right) \frac{J^{\mathcal{U}}}{d} \right] \quad (\text{A5})$$

$$\leq 1 \quad (\text{A6})$$

So,

$$\text{Tr}[J^{\mathcal{U}} \beta] = \frac{1}{d^2 \sum_i v_i} \text{Tr} [J^{\mathcal{U}} J^{\mathcal{E}' \circ \mathcal{U}}] \quad (\text{A7})$$

$$= \frac{1}{d^2 \sum_i v_i} \text{Tr} [\Phi_d^+ J^{\mathcal{E}'}] \quad (\text{A8})$$

Therefore, from the dual of the optimization problem of the generalized robustness, it holds that

$$R^+(\mathcal{U}) \geq \frac{1}{d^2 s} \text{Tr}[\Phi_d^+ J^{\mathcal{E}'}] \quad (\text{A9})$$

where s denotes the sum of positive coefficients of implementable operations in the decomposition of \mathcal{U} . \square

Appendix B: Proof of Theorem 2

Theorem 2 statement. Consider an n -qubit unitary \mathcal{U} with local partially depolarizing noise $\mathcal{E}^{\text{depol}}$ of the form

$$\mathcal{E}^{\text{depol}}(\rho) = \left(1 - \frac{3p}{4}\right) \rho + \frac{p}{4} (X\rho X + Y\rho Y + Z\rho Z), \quad (\text{B1})$$

acting on each qubit after the application of \mathcal{U} . The generalized robustness of \mathcal{U} is bounded by

$$R_{\text{depol}}^+(\mathcal{U}) \leq \left(\frac{4}{4-3p}\right)^n - 1. \quad (\text{B2})$$

Furthermore, when we consider the unitary to be d -dimensional (Kraus operators can be found in [42, 43]) and the noise to be d -dimensional depolarizing noise, then we get the following exact result for the generalized robustness of \mathcal{U} :

$$R_{\text{depol}}^+(\mathcal{U}) = \frac{d^2 - 1}{d^2 + p - d^2 p}. \quad (\text{B3})$$

Proof. The single-qubit depolarizing error $\mathcal{E}^{\text{depol}}$ with probability of error p acting on some qubit with quantum state ρ can be expressed as

$$\mathcal{E}^{\text{depol}}(\rho) = \left(1 - \frac{3p}{4}\right) \rho + \frac{p}{4} (X\rho X + Y\rho Y + Z\rho Z). \quad (\text{B4})$$

Using the above expression, we can express the identity channel acting ρ in terms of depolarizing noise as

$$\text{id}(\rho) = \frac{4}{4-3p} \mathcal{E}^{\text{depol}}(\rho) - \frac{p}{4-3p} (X\rho X + Y\rho Y + Z\rho Z) \quad (\text{B5})$$

Let us denote $X\rho X + Y\rho Y + Z\rho Z$ as $3\mathcal{N}(\rho)$. Since $\mathcal{U} = \text{id} \circ \mathcal{U}$, we get

$$\mathcal{U}(\rho) = \frac{4}{4-3p} \mathcal{E}^{\text{depol}} \circ \mathcal{U}(\rho) - \frac{3p}{4-3p} (\mathcal{N} \circ \mathcal{U}(\rho)) \quad (\text{B6})$$

If we let $\mathcal{I}_{\mathcal{E}}$ to be a continuous set of implementable operations, we get that $\mathcal{E}^{\text{depol}} \circ \mathcal{U} \in \mathcal{I}_{\mathcal{E}}$. Then using Eq. 26, we have

$$R^+(\mathcal{U}) \leq \frac{4}{4-3p} - 1 = \frac{3p}{4-3p}. \quad (\text{B7})$$

If we now consider \mathcal{U} to be an n -qubit unitary operation, and the depolarizing error to acting locally on each qubit after the application of \mathcal{U} , we get

$$R^+(\mathcal{U}) \leq \left(\frac{4}{4-3p}\right)^n - 1. \quad (\text{B8})$$

Next, for the d -dimensional case, we can express the d -dimensional depolarizing noise $\mathcal{E}_d^{\text{depol}}$ as

$$\mathcal{E}_d^{\text{depol}}(\rho) = \left(1 - \frac{d^2 - 1}{d^2} p\right) \rho + \text{other terms} \quad (\text{B9})$$

Then, based on the arguments above, we can express the identity channel in terms of the depolarizing noise, and get the upper bound on the generalized robustness of the d -dimensional unitary operation \mathcal{U} as

$$R^+(\mathcal{U}) \leq \frac{d^2 - 1}{d^2 + p - d^2 p}. \quad (\text{B10})$$

For the lower bound, let us define a positive semi-definite matrix β as follows

$$\beta := \frac{J^{\mathcal{U}}}{d^2 + p - d^2 p} \geq 0 \quad (\text{B11})$$

Now for any $Y = \mathcal{E}^{\text{depol}} \circ \mathcal{W} \in \mathcal{I}_{\mathcal{E}}$ where $\mathcal{W} \in \text{CPTP}(d)$, we have that

$$\text{Tr}[J^Y \beta] = p \text{Tr} \left[\frac{I \otimes I}{d} \frac{J^{\mathcal{U}}}{(d^2 + p - d^2 p)} \right] \quad (\text{B12})$$

$$+ (1-p) \frac{\text{Tr}[J^{\mathcal{W}} J^{\mathcal{U}}]}{d^2 + p - d^2 p} \quad (\text{B13})$$

$$\leq \frac{p}{d^2 + p - d^2 p} + \frac{(1-p)d^2}{d^2 + p - d^2 p} \quad (\text{B14})$$

$$= 1 \quad (\text{B15})$$

Therefore, for the defined β above, the conditions in Eq. (27) are satisfied. So, we get that

$$R^+(\mathcal{U}) \geq \text{Tr}[J^{\mathcal{U}} \beta] - 1 \quad (\text{B16})$$

$$= \frac{\text{Tr}[J^{\mathcal{U}} J^{\mathcal{U}}]}{d^2 + p - d^2 p} - 1 \quad (\text{B17})$$

$$= \frac{d^2 - 1}{d^2 + p - d^2 p} p. \quad (\text{B18})$$

And therefore, for the partially depolarizing noise, we get

$$R^+(\mathcal{U}) = \frac{d^2 - 1}{d^2 + p - d^2 p} p \quad (\text{B19})$$

□

Appendix C: Proof of Lemma 1 and Theorem 3

Lemma 1 statement. Given a single-qubit probabilistic error channel \mathcal{E} of the form

$$\mathcal{E}(\rho) = p\mathcal{N}(\rho) + (1-p)\rho, \quad (\text{C1})$$

acting on the qubit after the application of a single-qubit operation \mathcal{U} , the generalized robustness of \mathcal{U} is bounded by

$$R^+(\mathcal{U}) \leq \left(\frac{p}{1-p} \right) \quad (\text{C2})$$

Theorem 3 statement. Given the single-qubit dephasing error $\mathcal{E}^{\text{deph}}$ of the form

$$\mathcal{E}^{\text{deph}}(\rho) = \left(1 - \frac{p}{2}\right)\rho + \frac{p}{2}(Z\rho Z), \quad (\text{C3})$$

acting on the qubit after the application of a single-qubit operation \mathcal{U} , the generalized robustness of \mathcal{U} is equal to

$$R_{\text{deph}}^+(\mathcal{U}) = \frac{p}{2-p}. \quad (\text{C4})$$

Proof. The proof of Lemma 1 is based on expressing the identity channel as

$$\text{id}(\cdot) = \frac{1}{1-p}\mathcal{E}(\cdot) - \frac{p}{1-p}\mathcal{N}(\cdot) \quad (\text{C5})$$

which comes from the definition of the probabilistic error channel \mathcal{E} in Eq. (33). Using the above, the ideal unitary channel \mathcal{U} can be expressed as

$$\mathcal{U}(\cdot) = \frac{1}{1-p}\mathcal{E} \circ \mathcal{U}(\cdot) - \frac{p}{1-p}\mathcal{N} \circ \mathcal{U}(\cdot). \quad (\text{C6})$$

Then, from Eq. 26, we get

$$R_{\mathcal{I}_{\mathcal{E}}}^+(\mathcal{U}) \leq \frac{p}{1-p}. \quad (\text{C7})$$

For the proof of Thm. 3, we use the above result and get the upper bound on the generalized robustness of a unitary channel \mathcal{U} under partially dephasing channel $\mathcal{E}^{\text{deph}}$ (as defined in Eq. (35)) to be

$$R_{\text{deph}}^+ \leq \frac{2}{2-p}. \quad (\text{C8})$$

Now for the lower bound of Thm. 3, let $\mathcal{M} \in \text{CPTP}(2)$. The Choi matrix of \mathcal{M} under partially dephasing channel, that is the operation $\mathcal{E} \circ \mathcal{M}$, is given by

$$J^{\mathcal{E} \circ \mathcal{M}} = \text{id} \otimes \mathcal{E} \circ \mathcal{M}(\Phi^+) \quad (\text{C9})$$

$$= \left(1 - \frac{p}{2}\right) J^{\mathcal{M}} + \frac{p}{2} \text{id} \otimes Z (J^{\mathcal{M}}). \quad (\text{C10})$$

So, we can express the generalized robustness of a unitary channel under a partially dephasing channel as

$$\begin{aligned} R_{\text{deph}}^+(\mathcal{U}) &= \sup \text{Tr}[J^{\mathcal{U}}\beta] - 1 \\ \text{s.t. } 0 &\leq \left(1 - \frac{p}{2}\right) \text{Tr}[J^{\mathcal{M}}\beta] + \frac{p}{2} \text{Tr}[\text{id} \otimes Z (J^{\mathcal{M}})\beta] \leq 1, \\ \beta &\geq 0, \mathcal{M} \in \text{CPTP}(2), \end{aligned} \quad (\text{C11})$$

Now, let

$$\beta = \frac{1}{2(2-p)} J^{\mathcal{U}}, \quad (\text{C12})$$

then we have

$$\mathrm{Tr}[J^{\mathcal{M}}\beta] = \frac{1}{2(2-p)}\mathrm{Tr}[J^{\mathcal{M}}J^{\mathcal{U}}] = \frac{1}{2(2-p)}\mathrm{Tr} [((\mathcal{U}^T)^\dagger \otimes \mathcal{M}(\Phi^+)) \Phi^+] \quad (\text{C13})$$

and

$$\frac{1}{2(2-p)}\mathrm{Tr}[\mathrm{id} \otimes Z(J^{\mathcal{M}})J^{\mathcal{U}}] = \frac{1}{2(2-p)}\mathrm{Tr}[(\mathrm{id} \otimes Z)(\mathrm{id} \otimes \mathcal{M}(\Phi^+))(\mathcal{U}^T \otimes \mathrm{id})(\Phi^+)] \quad (\text{C14})$$

$$= \frac{1}{2(2-p)}\mathrm{Tr} [((\mathcal{U}^T)^\dagger \otimes \mathcal{M}(\Phi^+)) (\mathrm{id} \otimes Z(\Phi^+))] \quad (\text{C15})$$

For simplicity, let us denote $((\mathcal{U}^T)^\dagger \otimes \mathcal{M}(\Phi^+))$ by \mathbf{J} and check whether the constraint in Eq. C11 is obeyed.

$$\begin{aligned} \left(1 - \frac{p}{2}\right) \mathrm{Tr}[J^{\mathcal{M}}\beta] + \frac{p}{2} \mathrm{Tr}[\mathrm{id} \otimes Z(J^{\mathcal{M}})\beta] &= \frac{1}{2(2-p)} \left[\left(1 - \frac{p}{2}\right) (\langle 00|\mathbf{J}|00\rangle + \langle 00|\mathbf{J}|11\rangle + \langle 11|\mathbf{J}|00\rangle + \langle 11|\mathbf{J}|11\rangle) \right. \\ &\quad \left. + \left(\frac{p}{2}\right) (\langle 00|\mathbf{J}|00\rangle - \langle 00|\mathbf{J}|11\rangle - \langle 11|\mathbf{J}|00\rangle + \langle 11|\mathbf{J}|11\rangle) \right] \\ &= \frac{1}{2(2-p)} [\langle 00|\mathbf{J}|00\rangle + \langle 11|\mathbf{J}|11\rangle + (1-p)(\langle 00|\mathbf{J}|11\rangle + \langle 11|\mathbf{J}|00\rangle)] \end{aligned} \quad (\text{C16})$$

Now, $\langle 00|\mathbf{J}|00\rangle + \langle 11|\mathbf{J}|11\rangle \leq \mathrm{Tr}[\mathbf{J}] = 2$ and $\langle 00|\mathbf{J}|11\rangle + \langle 11|\mathbf{J}|00\rangle \leq \mathrm{Tr}[\mathbf{J}] = 2$. Therefore,

$$\left(1 - \frac{p}{2}\right) \mathrm{Tr}[J^{\mathcal{M}}\beta] + \frac{p}{2} \mathrm{Tr}[\mathrm{id} \otimes Z(J^{\mathcal{M}})\beta] \leq \frac{1}{2(2-p)} (2 + 2(1-p)) = 1 \quad (\text{C17})$$

and thus with the particular choice of β as in Eq. C12, the constraint in Eq. C11 is satisfied. Hence, we get that

$$R_{\text{deph}}^+ \geq \frac{2}{2-p}. \quad (\text{C18})$$

So, from Eq. C8 and C18, we have

$$R_{\text{deph}}^+ = \frac{2}{2-p}, \quad (\text{C19})$$

which completes the proof. \square

Appendix D: Alternate method to select gates for HEMRE

Given a maximum tolerable bias provided by the user, Δ_{fixed} , there can be several ways to select the gates which need to be approximated and for which the quasi-probabilistic decomposition need to taken into account. In the main text, we chose to approximate those gates which had the least generalized robustness. The advantage in using such a method was that we were able to maximize the number of gates to be approximated. However, if there are a lot of unique gates in the circuit, then sorting might be a time consuming process. In such a case, we can choose the first m gates such that the product of their generalized robustness does not go beyond the bound in Eq. (38). Another way can be to sort the gates in reverse order according to their generalized gates and approximate those gates which have the largest generalized robustness. Alternatively, we can sort based on the total generalized robustness of each unique gate in the circuit.

Below we present an algorithm to select gates to be approximated by sorting the gates by their generalized robustness in the decreasing order, that is, $s_1 \geq s_2 \geq \dots \geq s_N$. We index the gate accordingly, i.e., based on their generalized robustness, and not by their position in the circuit. So, the first gate will be the one with generalized robustness s_1 , second gate will be the one with generalized robustness s_2 , and so on. Note that this does not imply that $\gamma_1 \geq \gamma_2 \geq \dots \geq \gamma_N$. Also, in this case, we are assuming that there are several unique gates and so not relying on the frequency of the gates. This is often the case in parameterized circuits used in VQAs where different gates have different parameters [7]. Below, we provide an algorithm whose runtime scales as $O(N)$ and with which we can choose the decomposition of gates in the circuit such that we get a much reduced sampling overhead for estimating the expectation value up to the allowed bias. We denote total overhead by `tot_overhead` which is the product of

the generalized robustness of the approximated gates and the robustness of the remaining gates. We also define a two-valued variable called final_index which stores the final-index or the range of the operations which will be approximated. For instance, if $N = 5$ and final_index = $[2, 4]$, then only the second, third and fourth gates will be approximated.

```

1: tot_overhead  $\leftarrow \infty$ 
2: final_index =  $[0, 0]$ 
3: for  $j = (1 : N)$  do
4:   prod  $\leftarrow 1$ 
5:   s_incl  $\leftarrow 1$ 
6:   index =  $[0, 0]$ 
7:   for  $i = (j : N)$  do
8:      $s_m = s_{\text{incl}} * s_i$ 
9:     if  $s_m \leq \Delta_{\text{fixed}} - \epsilon + 1$  and  $i < N$  then
10:       $s_{\text{incl}} = s_m$ 
11:     else
12:       $prod = s_{\text{incl}} * \frac{\prod_{k=1}^N \gamma_k}{\prod_{k=j}^i \gamma_k}$ 
13:      index =  $[j, i]$ 
14:      if  $prod < tot\_overhead$  then
15:         $tot\_overhead = prod$ 
16:        final_index = index
17:      if  $i < N$  then
18:        break
19:      else
20:        return

```

Using final_index, we can then choose the gates that need to be approximated according to their generalized quasi-probability decomposition and for the remaining gates, we will use their quasi-probability decomposition. Chosen in this way, we will achieve a bias close to (and still less than or equal to) the allowed bias and a much reduced sampling overhead.

Appendix E: Numerical Analyses for mitigating errors from inhomogeneous Pauli noise

Here we present more numerical analyses that we conducted to compare the performance of EMRE with PEC. For our analyses, we use the SWAP-test with 7 qubits, and 140 gates. We tested the mitigation protocols under two noise models: the partially depolarizing noise model and the inhomogeneous Pauli noise model. The analysis of the comparison under the depolarizing noise is provided in the main text in Section V and the analyses of the results under inhomogeneous Pauli noise is given below. In addition to the analysis given in Section V, we also provide a table (see Table I) to quantitatively compare the expectation value estimates for few noise probabilities for PEC, EMRE, and HEMRE under partially depolarizing noise.

Noise probability \ EM (samples)	No EM	PEC(1000)	EMRE(1000)	HEMRE(1000)
0.01	0.3633	0.3636	0.4816	0.1134
0.005	0.248	0.2257	0.184	0.0974
0.001	0.0859	0.0645	0.0352	0.0460
0.0005	0.05273	0.0253	0.01309	0.024

TABLE I: Comparison of the bias from no EM, PEC, EMRE, and HEMRE under different depolarizing noise probabilities

To compare the performance of EMRE against PEC given inhomogeneous Pauli noise, we plot how the bias in the result increased as we increased the noise probability in the circuit, see Fig. 7. We used the SWAP test circuit and mitigated errors on single-qubit gates only. We left the error mitigation on two-qubit gates as we had limited computational power to obtain the decomposition of two qubit gates in terms of the implementable operations. For the analysis, we incremented the total noise probability by 0.0005, and distributed it among the X-, Y- and Z-noise by choosing randomly from the list: 0.0001, 0.0002, 0.0002. Refer to Table II for the list of the X-, Y-, and Z-noise probabilities as we increased the total noise probability. To generate the mean and standard deviation for a particular

Total noise probability	p_x	p_y	p_z
0.0005	0.0	0.0003	0.0002
0.001	0.0002	0.0004	0.0004
0.0015	0.0003	0.0004	0.0008
0.002	0.0006	0.0004	0.001
0.0025	0.0008	0.0005	0.0012
0.003	0.0009	0.0005	0.0016
0.0035	0.0009	0.001	0.0016
0.004	0.0009	0.0013	0.0018
0.0045	0.0011	0.0013	0.0021
0.005	0.0015	0.0013	0.0022
0.0055	0.0017	0.0013	0.0025
0.006	0.0020	0.0013	0.0027
0.0065	0.0022	0.0015	0.0028
0.007	0.0022	0.0017	0.0031
0.0075	0.0027	0.0017	0.0031
0.008	0.0030	0.0019	0.0031

TABLE II: Noise probabilities used for bias comparison in PEC and EMRE under inhomogeneous Pauli error channel

noise probability, we obtained 50 expectation values for each case: no EM used, with PEC, and with EMRE. When PEC or EMRE were deployed, the circuit was sampled 1000 times. From Fig. 7, we see that EMRE consistently performs better than PEC as the noise probability is increasing. Moreover, the standard deviation of EMRE is very small implying that the any expectation value obtained (by 1000 samplings (in this case)) will be very close to the mean indicating the reliability of EMRE.

For a more detailed analysis, in Fig. 8 and Fig. 9, we provide the distribution of the 50 estimates of the expectation values obtained when no EM was used, when PEC was used, and when EMRE was used for total noise probabilities of 0.005 and 0.0005, respectively. From the figures, we can clearly see that the spread of the estimates is very large when no EM is used thus there is no reliability in the result obtained. On the other hand, when PEC and EMRE are used, we see that the variances are reduced, and even more so for EMRE. We also see that for the sampling size of 1000, the (mean) bias from EMRE is much smaller than that of PEC. Lastly, we also provide a table (see Table III) to quantitatively compare the bias from PEC and EMRE for four different noise probabilities of inhomogeneous Pauli noise. We see that for low noise probabilities, EMRE outperforms PEC, and for noise probabilities where EMRE's bias is high, HEMRE gives better bias than PEC.

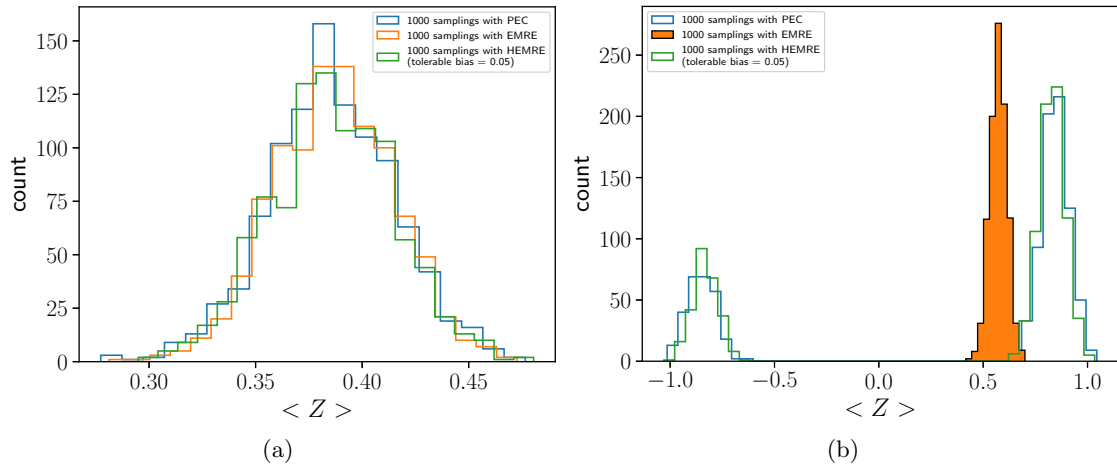


FIG. 6: (a) Expectation values and (b) Unbiased estimators of Z obtained after using PEC, EMRE and HEMRE each with 1000 samples, given depolarizing noise with noise probability of 0.002.

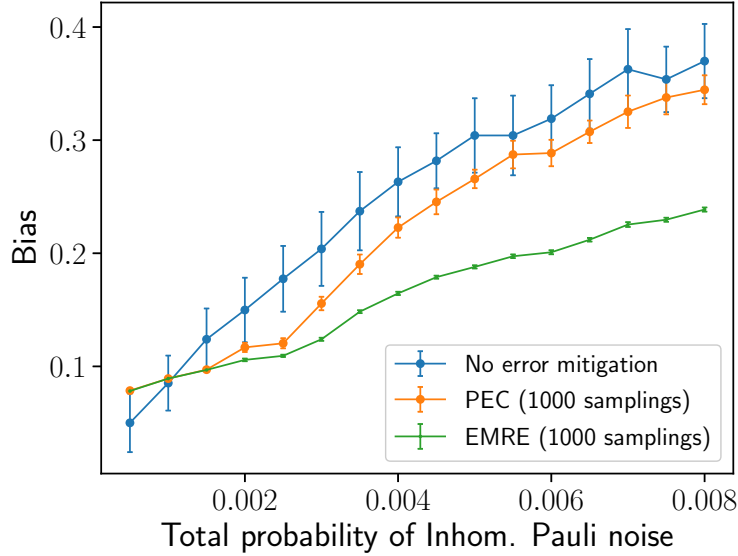


FIG. 7: Comparison of the performance of EMRE against PEC and no EM under the inhomogeneous Pauli noise. Note that for this comparison, we did not mitigate error on two-qubit gates.

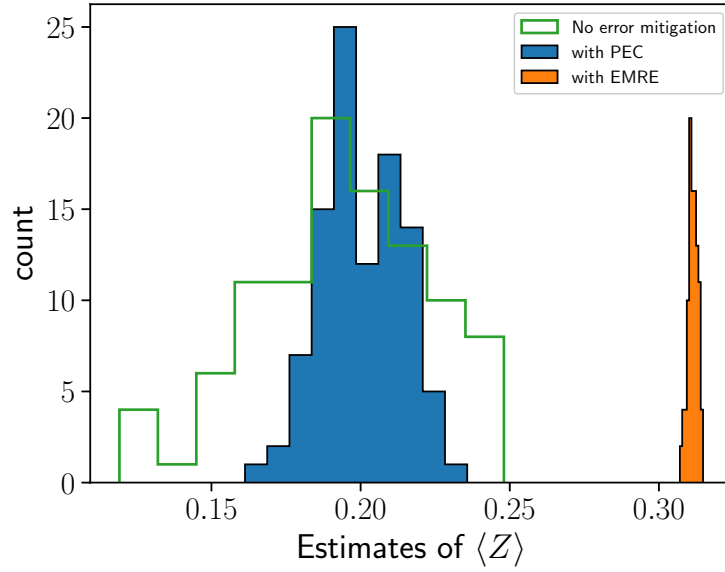


FIG. 8: Plot of the distribution of the 100 estimates of the expectation value of Z obtained without any error mitigation, with PEC, and with EMRE. In this plot, we considered inhomogeneous Pauli noise with probability of X-, Y-, and Z-error to 0.0005, 0.0005, and 0.004, respectively.

Noise probability	EM (samples)				
	No EM	PEC(1000)	PEC(10000)	EMRE(1000)	EMRE(2000)
0.009 (0.001, 0.002, 0.006)	0.414	0.3975	0.3831	0.4284	0.4280
0.005 (0.0005, 0.0005, 0.004)	0.3261	0.2982	0.2936	0.1910	0.1895
0.001 (0.0002, 0.0002, 0.0006)	0.0878	0.0737	0.0755	0.0443	0.0431
0.0005 (0.0001, 0.0001, 0.0003)	0.0332	0.0399	0.0419	0.0223	0.0216

TABLE III: Comparison of error obtained by using EMRE (performed with 1000 and 2000 samples) and PEC (performed with 1000 and 10000 samples) on C-SWAP circuit under the inhomogeneous Pauli noise error with different noise probabilities p_x , p_y and p_z for the X, Y, and Z error. Note that for these numerical simulation results, we did not mitigate errors on two-qubit gates.

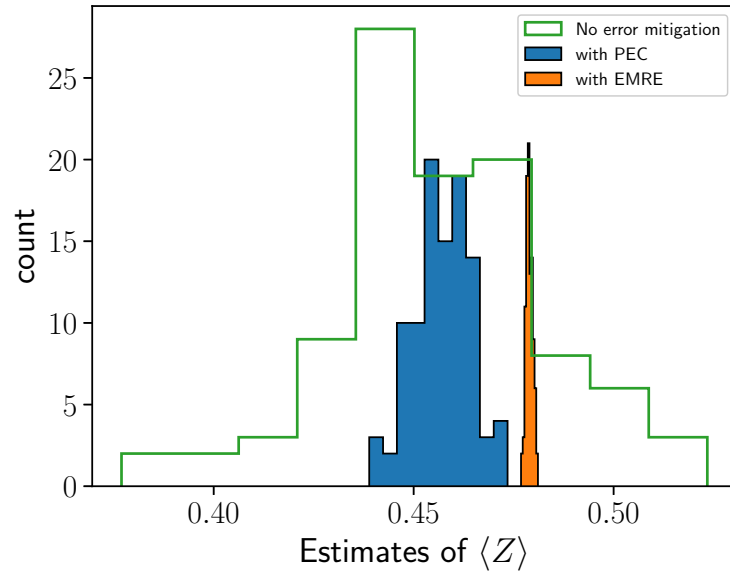


FIG. 9: Plot of the distribution of the 100 estimates of the expectation value of Z obtained without any error mitigation, with PEC, and with EMRE. In this plot, we considered inhomogeneous Pauli noise with probability of X-, Y-, and Z-error to 0.0001, 0.0001, and 0.0003, respectively.